GENERAL WETLAND SCIENCE

An Improved Model for Investigating Dual Effects of Vegetation Density Variations and Groundwater Level Fluctuations on Water Transport and Dissipation in Raised Field Wetlands

Yunlong Zhang [1,2] · Xuan Wang [1,2] · Dan Liu [1,2] · Yujun Yi [1,2] · Chunhui Li [2] · Qiang Liu [1] · Yanpeng Cai [1,3]

Abstract

An improved model for investigating dual effects of vegetation density variations and groundwater level fluctuations on water transport and dissipation in the soil-plant-atmosphere continuum (SPAC) of raised field wetlands was developed through combining the HYDRUS and the dual crop coefficient models. The results showed the following: (1) the improved model was reliable for soil water and evapotranspiration simulation. For soil water, the coefficient of determination (R^2) was above 0.68, the Nash-Sutcliffe efficiency coefficient (NSE) was above 0.53, and the relative deviation (R_e) was below 6%. For evapotranspiration, R^2, NSE and R_e were 0.83, 0.83 and 12.3%, respectively. (2) For the evapotranspiration, both vegetation densities variations and groundwater level fluctuation would affect it. (3) For 0%–60% density, the groundwater level fluctuation mainly contributed to changes in evaporation rather than transpiration. For 80%–100% density, it was transpiration. (4) For the soil water supplement and drainage, under different densities, the main water replenishment source in the same month was almost identical, but the main water drainage approach was inconsistent. (5) For the soil water balance, groundwater level fluctuations had an influence on it, while vegetation density variations did not. This study can provide an method for analyzing water transport in SPAC.

Keywords Improved HYDRUS model · Dual crop coefficient models · Vegetation density · Groundwater level · Water transport and dissipation

Introduction

In semi-arid areas, water resources are relatively scarce and ecosystems are fragile and highly prone to degradation, maintaining and restoring ecosystem health in semi-arid areas is important (Chesson et al. 2004; Cortina et al. 2011). Wetlands have an irreplaceable role in regulating climate, conserving water, and protecting biodiversity in such areas. Evapotranspiration is one of main ways of lose water of wetlands, which affects water balance and the stability of wetland ecosystems. Therefore, in soil-vegetation-atmosphere continuum (SPAC) of wetland, it is of great significance to study the evapotranspiration response to vegetation, groundwater and other conditions for revealing the mechanism of wetland water balance, water migration and water conservation and maintaining the stability of ecosystem.

As for impact factors of water transport and dissipation in SPAC of wetlands, some research reported that vegetation structure has a great impact on evapotranspiration, soil water dynamics, groundwater recharge and so on (Ludwig et al. 2005; Zhang and Schilling 2006; Chen et al. 2010). Fu et al. (2012) and She et al. (2014) suggested that shifting vegetation type and density could lead to a sustainable soil water-storage regime. Vegetation density is the common used indicator in the study of the vegetation structure, it is an indicator that cannot be ignored in the research of water transport and dissipation (Lortie and Turkington 2002; Jefferson 2004). In addition, due to water shortages and fragile ecosystems in semi-arid zones, to maintain the ecosystem health, some artificial ecological water replenishment projects (inter-basin or basin

✉ Xuan Wang
  wangx@bnu.edu.cn

1 State Key Laboratory of Water Environment Simulation, Beijing Normal University, Beijing 100875, China

2 Key Laboratory for Water and Sediment Sciences of Ministry of Education, Beijing Normal University, Beijing 100875, China

3 Beijing Engineering Research Center for Watershed Environmental Restoration and Integrated Ecological Regulation, School of Environment, Beijing Normal University, Beijing, China

water diversion measures to maintain the environment flow or ecological water requirement) have been instituted (Wang et al. 2013). Groundwater level fluctuations resulting from ecological water transfer projects affect both the physiological and ecological processes of vegetation as well as water transport and dissipation in the regional area (Karimov et al. 2014; Xu et al. 2016). Some studies demonstrated that groundwater level fluctuations had a significant impact on evapotranspiration (Gribovszki et al. 2008; Barreto et al. 2009; Fahle and Dietrich 2014). Therefore, performing an in-depth analysis of the law of water transport and dissipation of SPAC in raised field wetlands with vegetation density variations and groundwater level fluctuations is important.

Model simulation is an important method for ecological hydrological process simulations. Its advantage is that it can provide timely soil water content and evapotranspiration data and other information through setting boundary conditions based on field monitoring data. It also facilitates predictions and comparisons of diverse management schemes. In recent research, Soil Water-carrying Capacity for Vegetation (SWCCV) model, HYDRUS model, Simultaneous Heat and Water Transfer (SHAW) model, Soil-Water-Atmosphere-Plant (SWAP) model, and so on were widely used to analyze the processes and laws of water transport and dissipation in SPAC systems (Jiang et al. 2011; Li et al. 2014; She et al. 2014; Liu and Shao 2015; Amiri 2017). Among them, the HYDRUS model has flexible boundary conditions, standardized computer programs, a friendly user interface and convenience. HYDRUS has been widely used in the simulation of the transport and dissipation of water and solutes in SPAC systems (Mastrocicco et al. 2010). However, the HYDRUS model cannot evaluate vegetation density variations, thus preventing quantitative analysis of the transport and dissipation processes of water at different vegetation densities. Therefore, we should consider adding other modules to adjust the HYDRUS model. The crop coefficient (K_c) is one of the most important approaches to obtain ET. The crop coefficient approaches consist of single and dual coefficient approaches. The dual crop coefficient (DualKc) approach can partition ET into E and T, it can also be used to estimate effects of rainfall, vegetation density and mulch use on soil water (Li and Ma 2019). The dual crop coefficients (DualKc) model can quantify the effect of vegetation density variations on evapotranspiration, while combining the HYDRUS model and DualKc module can provide an analysis of effects of vegetation density variations on transport and dissipation of water that included evapotranspiration, water replenishment and drainage, and soil water balance; however, the combination of these modules has not been studied yet by researchers.

The overall aims of this study were to construct an improved model for an investigation into how variations of the wetland vegetation structure and groundwater levels would affect transport and dissipation of water that included evapotranspiration, water replenishment and drainage, and soil water balance. First, we constructed an improved model that combined the HYDRUS and dual crop coefficients (DualK$_c$) models, that can be used to simulate different vegetation density conditions. Second, the effects of vegetation density variations and groundwater level fluctuations on water transport and dissipation in SPAC systems were analyzed through the improved model. The research results clarified the responses of transport and dissipation of water in the SPAC to the variations in the vegetation pattern and groundwater variations in Lake Baiyangdian. The main innovations of this study include two aspects. First, for the simulation of water transport and dissipation at different vegetation densities, most of the models cannot achieve vegetation density regulation (Fu et al. 2012; Wang et al. 2012a; She et al. 2014). This study combines HYDRUS (version 4.16.0110) and the DualKc module to solve this problem. Second, for measuring the complexity of water transport and dissipation in semi-arid wetlands, most studies do not simultaneously analyze the effects of vegetation density variations and groundwater level fluctuations on water transport and dissipation. This study performs a new joint model for in-depth analysis of the relationships among the vegetation structure, groundwater fluctuation, and water transport and dissipation. This research could provide the foundation technical support for water security, water conservation and decision-making for the quantitative management of the ecosystem.

Study Area and Data Acquisition

Lake Baiyangdian (38°43′–39°02′N and 115°38′–116°07′E) in Xiong'an New Area (Fig. 1) is the largest freshwater lake in the northern China plain. The regional climate is warm temperate continental monsoons. It lies in the middle reaches of the Daqing River basin and discharges into the Bohai Gulf, Yellow Sea. It is a grass-type shallow lake consisting of 143 islands and 67 km^2 of *Phragmites australis* (*P. australis*) marshes with a 31,200 km^2 catchment. The lake surface area is 366 km^2, and the average amount of water inflow is 908 million m^3 (Wang et al. 2014a, 2014b). There are natural low-lying depressions and *P. australis* marshes (Wang et al. 2012b). The lake is a source of livelihood for more than 200,000 inhabitants around its shore via agriculture, fishing, tourism, transportation and reed/lotus farming (Zhong et al. 2005).

P. australis is one of the most widespread wetland plant species on earth and is the main species used in wetlands (Brix et al. 2001; Borin et al. 2011). It plays a non-negligible role in wetland ecosystem. However, *P. australis* is one of the most water-intensive plants and severely deplete water in limited rainfall semi-arid and severe shortage of natural water resources regions. Some researches show that the evapotranspiration of *P. australis* dominated shallow lakes was one to
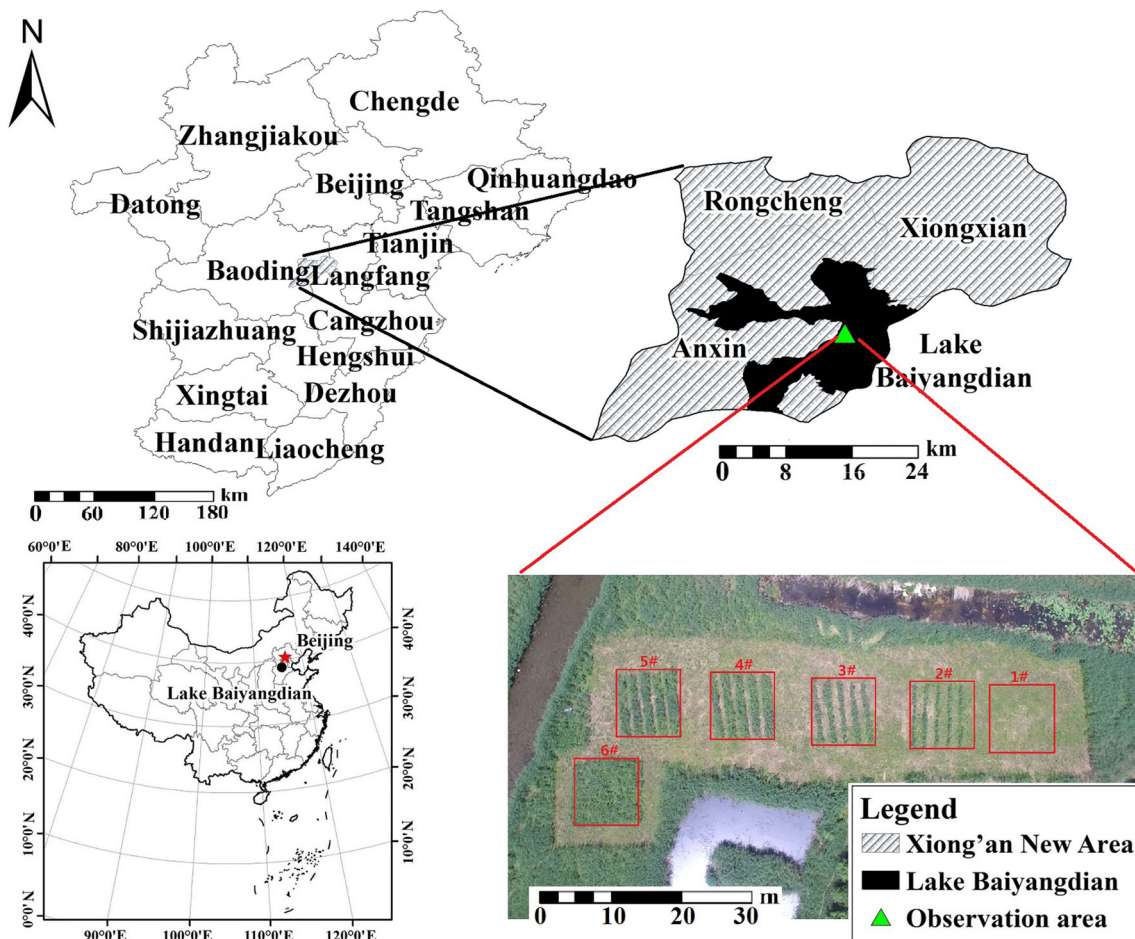
Fig. 1 Geographical location of the study area

seven times as high as the evaporation of water bodies without vegetation covered (Baird 1999; Zhou and Zhou 2009).

Massive reservoirs construction in upstream regions of the lake catchment has caused water shortage and worsened the lake hydrology by cutting off virtually all river discharge into the lake (Moiwo et al. 2010). Simultaneously, the lake is in a semi-arid area with a low annual precipitation of 550 mm over 7–9 months contributing 80% of the total precipitation, while the inter-annual amount of water greatly fluctuates. The main source of the water supply is the upstream ecological water supply, the groundwater level in the area is usually affected by the upstream ecological water supply. Thus, the groundwater level is mainly affected by human activities. The fluctuation between years usually lead to significant variations in evapotranspiration in the region. Hence analyzing water transport and dissipation of SPAC with vegetation density variations and groundwater level fluctuations is important to address severe ecological degradation (Karimov et al. 2014).

The observation area was located at raised fields, the middle area of Lake Baiyangdian, which was dominated by *P. australis* in natural conditions. There were six plots for 0%, 20%, 40%, 60%, 80% and 100% *P. australis* density, with each plot being 10 × 10 m and 5 m interval between plots (Fig.

1). Taking the natural condition of *P. australis* in the area *as* 100% density, it is about 40 plants /m^2. In the research, density management in each plot was achieved mainly through the strip cut method every 10 days. Joint monitoring of hydrology and meteorology elements was carried out. An observation tube of the Diviner 2000 soil moisture rapid measurement system (Sentek, Australia), a groundwater level observation well, a micro weather station and an eddy covariance system (LI-COR, USA) were installed. Thus, the monitoring elements included the 0–120 cm soil water content, the groundwater level, the original soil, an artificial vegetation survey (vegetation height, and so on), evapotranspiration, the rainfall temperature and other meteorological data. The monitoring period was from May 16, 2018, to September 30, 2018, covering the complete growing period of *P. australis*, and the monitoring intervals were 15 days. The micro weather station was automatically observed, and the observation frequency was 1 h. These data provide support for the construction of the numerical simulation.

In Lake Baiyangdian, the growth season of *P. australis* was from May to October, 2018. During the whole growing season of 2018 (Fig. 2), the total rainfall was 345.5 mm and was mainly concentrated in July and August, contributing

approximately 88% of the total rainfall. The highest daily temperature was 31.7 °C (August), while the daily average temperature was 23.4 °C. The vapor pressure varied from 0.77 to 3.94 KPa, and total solar radiation during the growing season was 2885.26 MJ/m². Groundwater level fluctuations are shown in Fig. 2(e). In general, from May to June, the groundwater level continued to decrease because there was less rainfall in May and June and a large amount of water was consumed in the early stages of *P. australis* growth. However, from June to August, the groundwater level continued to rise with the increased rainfall and elevated upstream water levels.

Improvement of the Water Transport and Dissipation Model Based on the HYDRUS Model

Combination of HYDRUS and Dual Crop Coefficient Models

The soil of the observation area was mainly sandy loam, which has strong permeability and does not easily produce subsurface flow. The area terrain was relatively flat, slightly

inclined from west to east, with a natural slope of 1 / 200–1 / 2000. Thus, the soil water in the unsaturated layer mainly moved vertically, and the lateral runoff in the saturated aquifer was low. Therefore, water transport and dissipation in the wetland SPAC system mainly considers the vertical dimension in the observation area.

Since the HYDRUS model cannot simulate water transport and dissipation at different vegetation densities, we combined the HYDRUS model and the dual crop coefficient model to develop a new model, called the HYDRUS-DualKc model. The combined method between the HYDRUS and DualKc models are shown in Fig. 3. First, according to meteorological data and the vegetation density, the dual crop coefficient model calculated the potential vegetation transpiration (T_p) and potential soil evaporation (E_p) at different vegetation densities, i.e., 0%, 20%, and so on. Second, E_p and T_p were input into the HYDRUS module as the upper boundary condition, with the groundwater level as the lower boundary condition. Finally, the improved model simulated the water transport and dissipation in the SPAC system, such as the actual vegetation evaporation (T_a), the actual soil transpiration (E_a) and the water balance at different vegetation densities and fluctuating groundwater levels. Through combining the HYDRUS
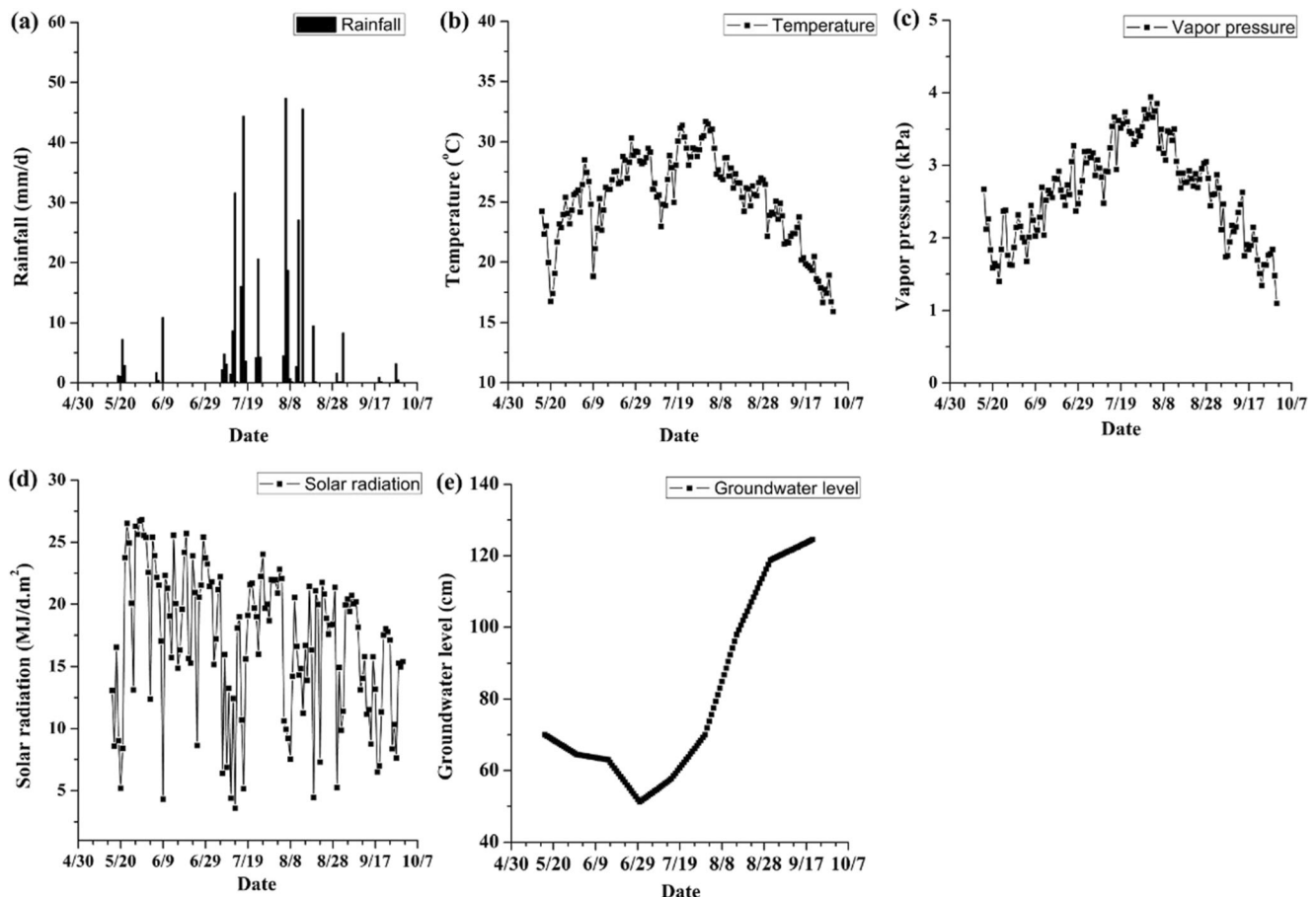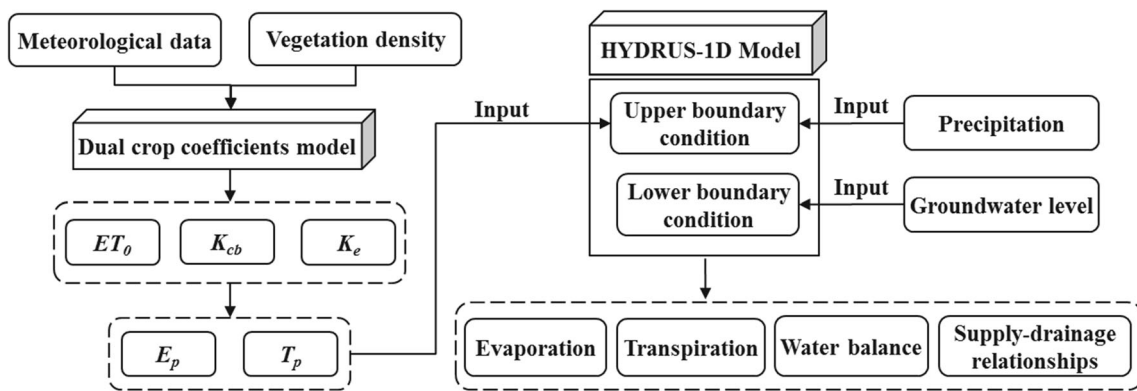

Fig. 2 Diurnal variations of rainfall, temperature, vapor pressure, solar radiation and groundwater level

Fig. 3 Improved model with the combination of the HYDRUS and dual crop coefficient models. (ET_0 is the reference crop evapotranspiration; K_{cb} is the basal crop coefficient of vegetation transpiration; K_e is the coefficient for soil evaporation; T_p is potential vegetation transpiration; E_p is potential soil evaporation)

Model Composition

HYDRUS Model

Richard's equation based on Darcy's law and the law of conservation of mass were used to simulate the soil water flow in the HYDRUS model and can be defined as follows:

$$\frac{\partial \theta}{\partial t} = \frac{\partial}{\partial x}\left[K\left(\frac{\partial h}{\partial x} + \cos\alpha\right)\right] - S(x,t) \tag{1}$$

where h is the pressure head, cm; θ is the volumetric water content of soil, cm^3·cm^{-3}; K is the hydraulic conductivity of soil water, cm·d^{-1}; α is the angle between the flow direction and vertical direction, so that $\alpha = 0°$ is the vertical flow or $\alpha = 90°$ is the horizontal flow; $S(x,t)$ is the source-sink term, cm^3·cm^{-3}·d^{-1}, i.e., the amount of water absorbed by the root from the unit volume of soil per unit time; t is the time, day; and x is the vertical soil depth, cm, with upward as the positive direction.

The amount of water absorbed by the root per unit volume of soil per unit time is reflected by the root water absorption rate, which is calculated by the Feddes model as follows:

$$A(h,x) = \alpha(h)b(x)T_p \tag{2}$$

where $A(h,x)$ is the root water absorption rate, cm·d^{-1}; T_p is the potential transpiration rate, cm·d^{-1}; $b(x)$ is the normalized water uptake distribution; and $a(h)$ is the root-water uptake water stress response function, $0 \le \alpha \le 1$, and can be defined as follows:

$$\alpha(h) = \begin{cases} \dfrac{h-h_4}{h_3-h_4} & h_4 < h \le h_3 \\ 1 & h_3 < h \le h_2 \\ \dfrac{h-h_1}{h_2-h_1} & h_2 < h \le h_1 \\ 0 & h \le h_4 \ \ h > h_1 \end{cases} \tag{3}$$

where h_1, h_2, h_3 and h_4 represent the plant anaerobiosis point (cm), the plant optimum moisture point (cm), the water stress point (cm) and the crop wilting point pressure head (cm), respectively. Water uptake is considered to occur at the optimal between pressure heads h_2 and h_3, whereas for the pressure head between h_3 and h_4 (or h_1 and h_2,), water uptake linearly decreases (or increases) with h.

The root water absorption distribution function $b(x)$ can be expressed as a function of relative depth using the following formula provided by Hoffman and Van Genuchten (Hoffman and Genuchten 1983):

$$b(x) = \begin{cases} \dfrac{1.6667}{L_R} & x > L-0.2L_R \\ \dfrac{2.0833}{L_R}\left(1-\dfrac{L-x}{L_R}\right) & x \in (L-L_R; L-0.2L_R) \\ 0 & x < L-L_R \end{cases} \tag{4}$$

where L is the x-coordinate of the soil surface, cm; L_R is the root depth, cm; and x is the x-coordinate of the soil profile, cm. The bottom of the soil profile is located at $x = 0$ and the soil surface at $x = L$.

According to the above formula, the actual transpiration can be calculated using the following formula:

$$T_a = \int_{L_R} A(h,x)dx = T_p \int_{L_R} \alpha(h)b(x)dx \tag{5}$$

where L_R is the root depth, cm; T_p is the potential transpiration rate, cm·d^{-1}; $b(x)$ is the normalized water uptake distribution; and $a(h)$ is the root-water uptake water stress response function.

For annual vegetation, a growth model is required to simulate the change in rooting depth with time. In the HYDRUS model, $L_R(t)$ can be defined as follows:

$$L_R(t) = \frac{L_m L_0}{L_0 + (L_m - L_0)e^{-rt}} \quad (6)$$

where L_0 is the initial value of the rooting depth at the beginning of the growing season, cm; r the growth rate, cm·d^{-1}. The growth rate is calculated either from the assumption that 50% of the rooting depth will be reached after 50% of the growing season has elapsed or from given data.

Dual Crop Coefficient Model and Density Regulation Method

The World Food and Agriculture Organization (FAO) proposed the dual crop coefficient model and split the single crop coefficient K_c into the basic crop coefficient K_{cb} for vegetation transpiration and the evaporation coefficient K_e for soil evaporation. Many studies have shown that although the dual crop coefficient model was more complicated than the single crop coefficient, it can be used to deal with some problems. These problems include natural sparse vegetation, and the FAO-56 dual crop coefficient model has thus been adopted and evaluated over several sparse crops (Goodwin et al. 2006; Poblete-Echeverria and Ortega-Farias 2013; Zhao et al. 2015). Therefore, the model can calculate evapotranspiration at different densities, and the accuracy of water transport and dissipation is improved by using the dual crop coefficient model. The dual crop coefficient model can be written as follows:

$$ET_c = (K_{cb} + K_e)ET_0 = K_{cb}ET_0 + K_eET_0 = T_p + E_p \quad (7)$$

where ET_c is the vegetation evapotranspiration under standard conditions when no limitations are placed on crop growth or evapotranspiration, i.e., the potential evapotranspiration of vegetation; K_{cb} is the basal crop coefficient of vegetation transpiration; K_e is the coefficient for soil evaporation; ET_0 is the reference crop evapotranspiration, which is calculated according to the Penman-Monteith formula by FAO; T_p is potential vegetation transpiration; and E_p is potential soil evaporation.

The K_{cb} recommended values for different vegetation can be found in the FAO56 document (Allen et al. 1998). Since the vegetation density has an impact on crop coefficients, simulation of the effect of vegetation density variations on water transport and dissipation was achieved by adjusting crop coefficients for the middle and end season stages of vegetation (called as $K_{cb\ mid}$ and $K_{cb\ end}$, respectively) in the model. According to the calculation method suggested by FAO crop evapotranspiration document (Allen et al. 1998), crop coefficients for *P. australis* in the middle season stage corresponded to June to August, and those in the end season stage corresponded to August to September. For the middle season

stage, the adjustment of $K_{cb\ mid}$ with different vegetation densities can be estimated similar to a procedure used by Ritchie (Ritchie 1972) as follows:

$$K_{cb\ mid} = K_{c\ min}$$
$$+ (K_{cb\ full} - K_{c\ min})\left(1 - \exp(-0.7LAI_{dense}D^a)\right) \quad (8)$$

where $K_{cb\ mid}$ is the estimated K_{cb} during the mid-season when vegetation densities are lower than under full cover conditions; $K_{c\ min}$ is the minimum K_c for bare soil, $K_{c\ min} = 0.15$–0.20; LAI_{dense} is LAI for a particular plant species under normal dense or pristine growing conditions, which can be obtained from various physiological sources and textbooks on crops and vegetation; D is the vegetation density; a is the correction factor, and $a = 0.5$ when the population is formed from vigorous growing plants and $a = 1$ when plants are less vigorous; and $K_{cb\ full}$ is the estimated K_{cb} during the mid-season for vegetation having full ground cover or LAI > 3 and can be calculated as follows:

$$K_{cb\ full} = K_{cb\ mid\ Table}$$
$$+ [0.04(u_2 - 2) - 0.004(RH_{min} - 45)]\left(\frac{h}{3}\right)^{0.3} \quad (9)$$

where $K_{cb\ mid\ Table}$ is $K_{cb\ mid}$ with a full coverage of vegetation, for more information refer to Table 17 in the FAO56 document (Allen et al. 1998); u_2 is the mean value for wind speed at 2 m height during the mid-season, m s^{-1}; RH_{min} is the mean value for the minimum daily relative humidity during the mid-season, %; and h is the mean maximum plant height, m.

For the late season stage, K_{cb} begins to decrease until it reaches $K_{cb\ end}$ at the end of the growing period. The values of $K_{cb\ end}$ can be scaled from $K_{cb\ mid}$ in proportion to the health and leaf condition of the vegetation at the end of the growing season and according to the length of the late season period.

The soil evaporation coefficient K_e is used to describe the evaporation component in ET_c. When soil is wet after rainfall or irrigation, evaporation from soil occurs at the maximum rate and K_e is the maximum value. The K_e value decreases when the soil surface is dry, and $K_e = 0$ when the total evaporable water is zero.

$$K_e = (K_{c\ max} - K_{cb}) \leq f_{ew}K_{c\ max} \quad (10)$$

where K_{cb} is the basal crop coefficient; f_{ew} is the fraction of the soil that is both exposed and wetted, i.e., the fraction of the soil surface from which most evaporation occurs; and $K_{c\ max}$ is the maximum value of K_c following rain or irrigation, and $K_{c\ max}$ ranges from approximately 1.05 to 1.30 and can be calculated using the following formula:

$$K_{c\ max} = \max\left(\left\{1.2 + [0.04(u_2-2)-0.004(RH_{min}-45)]\left(\frac{h}{3}\right)^{0.3}\right\}, \quad \{K_{cb} + 0.05\}\right) \qquad (11)$$

where h is the mean maximum plant height during the calculation period (initial, development, mid-season, or late-season), m; K_{cb} is the basal crop coefficient; RH_{min} is the mean value for daily minimum relative humidity; and u_2 is the mean value for daily wind speed at a 2 m height, m s^{-1}.

Initial and Boundary Conditions

According to the combined method for HYDRUS and DualKc (Fig. 3), we established an improved model in the observation area, and the upper and lower boundary conditions of the model were set to the atmospheric BC with the surface layer and variable pressure head, respectively. The upper boundary included rainfall, potential evaporation and potential transpiration. The lower boundary was only groundwater level. Variations of rainfall and groundwater level in 2018 are shown in Fig. 2. The initial condition was the vertical distribution of the 0–120 cm soil water content on May 16, 2018.

Using Eqs. (8) and (10), the dual crop coefficients were calculated for the different vegetation densities (0%, 20%, 40%, 60, 80% and 100% density). From bare lands to lands with a 20% vegetation density, the basic crop coefficients (K_{cb}) and soil evaporation coefficients (K_e) varied the most among the lands with various densities. Using eq. (7), the potential transpiration (T_p) and potential evaporation (E_p) for each *P. australis* density were calculated in 2018. The potential transpiration showed a single peak trend, the highest daily potential transpiration was 5.96 mm/d (July 21) at 100% density of *P. australis*, and the highest daily potential evaporation was 5.23 mm/d (June 27) under bare soil conditions and showed a significant decreased with *P. australis* growth. The daily potential evaporation remained at less than 1 mm/d between June 5 and September 5 but significantly increased at the end of the growth of *P. australis* (September).

Model Evaluation

In the observation area, 0-120 cm soil water is measured twice a month and 10 cm interval. 50% of the measured data quantity for calibration, and 50% of the measured data quantity for verification. The soil moisture measured data on May 31, June 30, July 31, and August 31, 2018 were used for model parameter calibration. The soil moisture measured data on June 15, July 15, August 15, and September 20, 2018 were used for model validation. Three statistics were used to evaluate the model performance: the coefficient of determination (R^2), the Nash-Sutcliffe efficiency coefficient (NSE) and the relative deviation (Re).

$$R^2 = \left[\frac{\sum\limits_{i=1}^{n}\left(S_i-\overline{S}\right)\left(M_i-\overline{M}\right)}{\sqrt{\left[\sum\limits_{i=1}^{n}\left(S_i-\overline{S}\right)^2\right]\left[\sum\limits_{i=1}^{n}\left(M_i-\overline{M}\right)^2\right]}}\right]^2 \qquad (12)$$

$$NSE = 1-\frac{\sum\limits_{i=1}^{n}\left(M_i-S_i\right)^2}{\sum\limits_{i=1}^{n}\left(M_i-\overline{M}\right)^2} \qquad (13)$$

$$Re = \frac{(S_i-M_i)}{M_i} \times 100\% \qquad (14)$$

where S_i and M_i are the simulated and observed soil water contents for the *ith* observation point, respectively; $\overline{S}$ and $\overline{M}$ are the averages of simulated and observed soil water contents, respectively; and n is the number of soil water content observations.

Results and Discussion

Model Calibration and Validation

The calibrated soil parameters were inversely estimated by the Marquardt-Levenberg type algorithm in HYDRUS and are presented in Table 1. The predominant soil in the study area was sandy loam, and the calibrated parameters were basically similar to the soil parameters of sandy loam given by the US Department of Agriculture. For different densities, three statistics for the measured and simulated values of the soil water content during calibration and validation showed that there was a close agreement between the measured and simulated soil water contents (Table 2). During the calibration, under each density condition, R^2 was above 0.68, NSE was above 0.53, and R_e was below 6%. During the validation, all R^2 was 0.746–0.850, NSE was 0.550–0.816, and R_e was 2.308%–5.333%. In general, the simulation accuracy during the verification was slightly worse than that during the calibration, but the simulation results were still good. A comparison of the measured and simulated soil water contents is shown in Fig. 4 and Fig. 5. In general, these results showed that the model had a high simulation accuracy for soil water content variations.

Table 1 Summary of the calibrated parameters of the model

Density	Depth/cm	θ_r/(cm³/cm³)	θ_s/(cm³/cm³)	α/cm⁻¹	n	K_s/(cm/d)	l
0%	0–10	0.04	0.46	0.020	1.3	30	0.5
	10–20	0.04	0.47	0.015	1.3	50	0.5
	20–40	0.04	0.48	0.020	1.3	50	0.5
	40–120	0.04	0.49	0.017	2.0	40	0.5
20%	0–10	0.04	0.46	0.029	1.3	30	0.5
	10–20	0.04	0.47	0.015	1.3	50	0.5
	20–40	0.04	0.48	0.020	1.3	50	0.5
	40–120	0.04	0.49	0.017	2.0	40	0.5
40%	0–10	0.04	0.46	0.018	1.9	30	0.5
	10–20	0.04	0.46	0.014	1.9	30	0.5
	20–40	0.03	0.48	0.020	1.3	50	0.5
	40–120	0.04	0.48	0.017	1.9	40	0.5
60%	0–10	0.04	0.46	0.029	1.9	30	0.5
	10–20	0.04	0.46	0.014	1.5	30	0.5
	20–40	0.03	0.48	0.020	1.3	50	0.5
	40–120	0.04	0.48	0.017	1.9	40	0.5
80%	0–10	0.02	0.47	0.022	1.3	40	0.5
	10–20	0.04	0.46	0.030	2.0	30	0.5
	20–40	0.02	0.47	0.040	1.4	40	0.5
	40–120	0.04	0.469	0.020	1.3	40	0.5
100%	0–10	0.04	0.47	0.030	1.4	30	0.5
	10–20	0.04	0.47	0.037	2.0	50	0.5
	20–40	0.02	0.47	0.020	1.4	40	0.5
	40–120	0.04	0.469	0.020	1.3	50	0.5

θ_r is residual soil water content; θ_s is saturated soil water content; α is parameter in the soil water retention function; n is exponent in the soil water retention function; K_s is saturated hydraulic conductivity; l is pore-connectivity parameter

As an important parameter, $K_{cb\ mid\ Table}$ (Eq. (9)) played an important role in determining the crop coefficient and soil evaporation coefficient under different density conditions and growth stages. However, in the FAO evapotranspiration document, the $K_{cb\ mid\ Table}$ reference value for *P. australis* was not given, which prevented the in-depth calculation and

Table 2 Simulation accuracy of the model during calibration and verification

|	Density	R^2	NSE	Re (%)
Calibration	0%	0.683	0.526	2.617
	20%	0.811	0.637	3.042
	40%	0.828	0.728	3.735
	60%	0.930	0.888	3.175
	80%	0.929	0.910	3.207
	100%	0.895	0.856	5.811
Validation	0%	0.746	0.550	2.308
	20%	0.800	0.555	2.997
	40%	0.766	0.627	3.103
	60%	0.850	0.766	2.769
	80%	0.828	0.816	3.468
	100%	0.817	0.804	5.333

R^2 is the coefficient of determination; NSE is the Nash-Sutcliffe efficiency coefficient; Re is the relative deviation

analysis of evapotranspiration changes of reed communities. Based on the evapotranspiration measurement data of full-cover *P. australis* in Baiyangdian, the suitable $K_{cb\ mid\ Table}$ for Baiyangdian area was determined. Table 3 showed that when $K_{cb\ mid\ Table} = 2.3$ the simulation accuracy was the best. Comparison of the simulated and measured evapotranspiration for full-cover *P. australis* is shown in Fig. 6. The improve HYDRUS-DualKc model was reliable for evapotranspiration simulation. In Baiyangdian, the $K_{cb\ mid\ Table}$ value of full-cover *P. australis* was 2.3.

Analysis of Water Transport and Dissipation in the Interface of SPAC Systems with Different Vegetation Densities

Vegetation density variations can change the ratios between vegetation cover and open water or the ground, which would ultimately alter plant species distributions, community structures and the physiological processes of species and may also have an impact on water consumption of the wetlands and partition evapotranspiration into the evaporation and transpiration constituents (Herbst and Kappen 1999; Drexler et al. 2004). Using the improved HYDRUS-DualKc model, the vertical water transport and dissipation in *P. australis* of different densities was simulated. The composition of the water flux in the SPAC system interface is shown in Table 4.
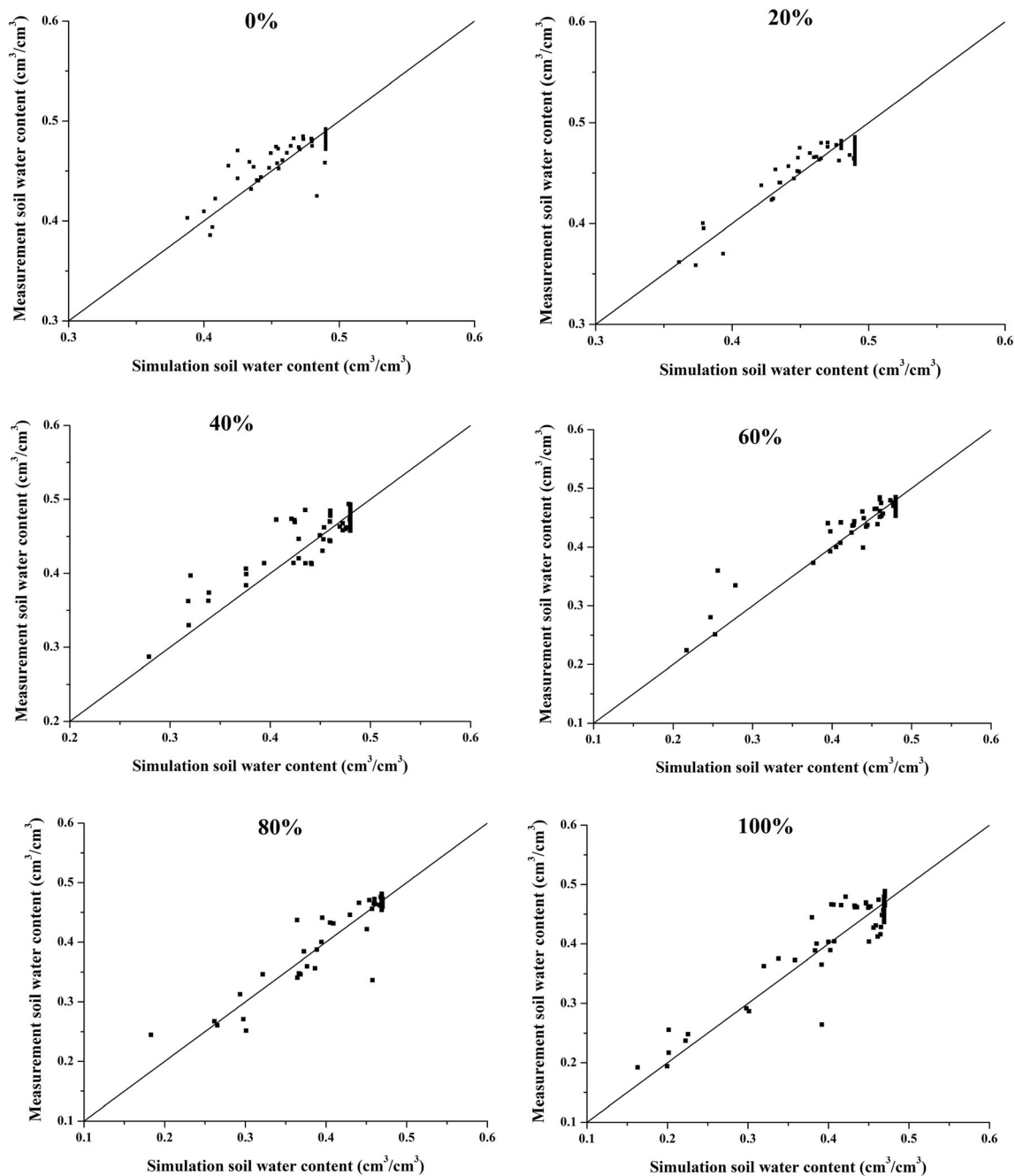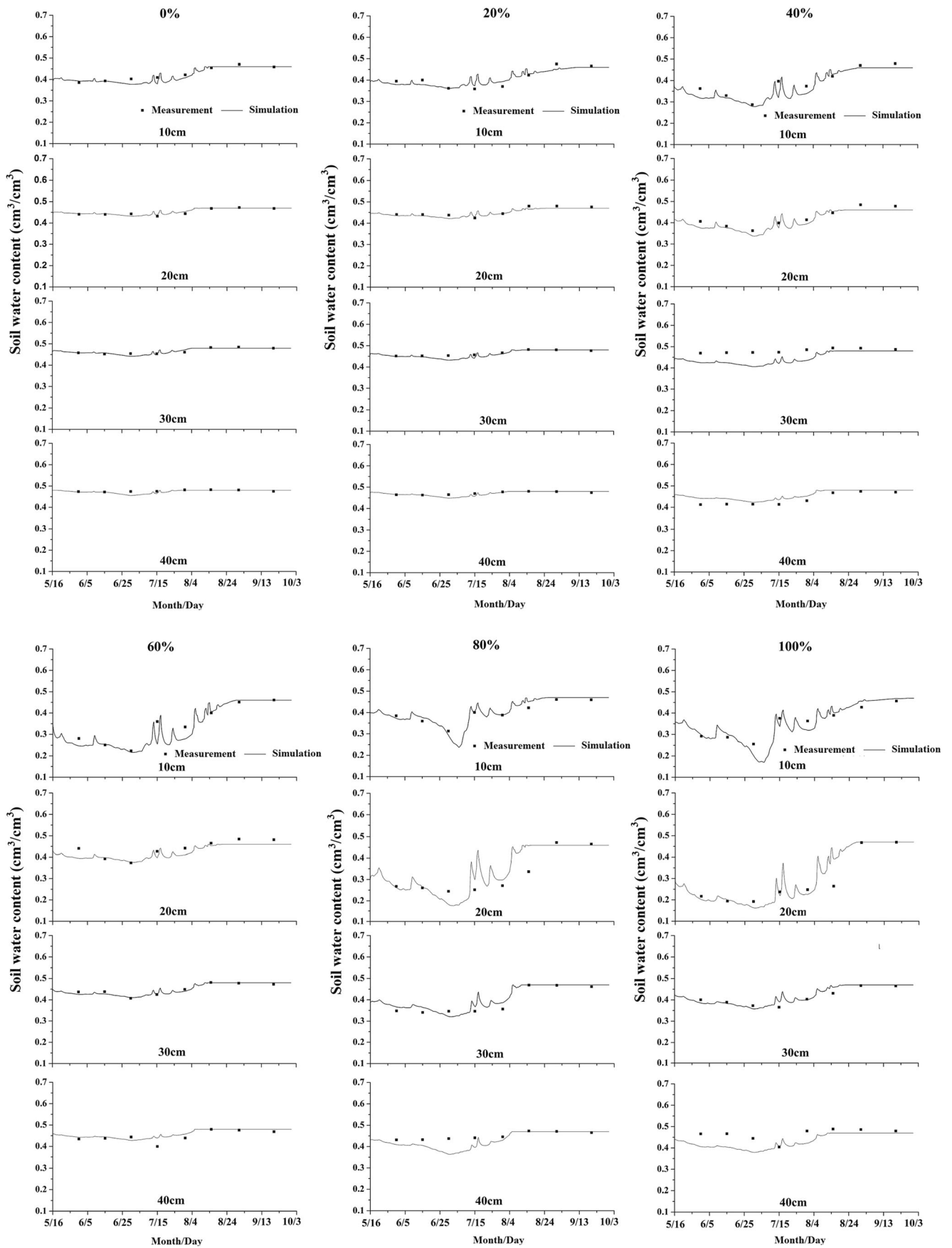
Fig. 4 Comparisons of the simulated and measured soil water contents in the profile of 0–120 cm for different densities. (The solid line indicates a 1:1 line; the percentage above each figure represents the *P. australis* density (%))

Evapotranspiration in Lake Baiyangdian included plant transpiration and soil evaporation. The bare land was dominated by soil evaporation, and the total amount of evaporation was 550 mm. Under the 40% density condition, during the growing season, the amount of transpiration was nearly equal to the soil evaporation (approximately 380 mm). However, vegetation transpiration was dominant in the growing season from 60%–100% densities of *P. australis*. The density and proportion of transpiration in evapotranspiration showed a positive

correlation. For 100% density, the proportion of transpiration was the highest and transpiration (1130 mm) was 20 times soil evaporation (48 mm). By comparing actual evapotranspiration at different *P. australis* densities, a significantly increasing trend in total actual evapotranspiration with the increasing vegetation density was observed (Table 4). The high evapotranspiration rate showed that the groundwater levels were suitable for *P. australis* growth in raised fields. In general, at the current groundwater level, sufficient water levels were

◄ Fig. 5 Comparisons of the simulated and measured soil water contents in various depths for different densities. (The percentage above figure represents the *P. australis* density (%); the number below the figure represents the soil depth (cm))

(a)

beneficial to vegetation transpiration, and the actual transpiration values of *P. australis* under various density conditions all reached their potential transpiration values.
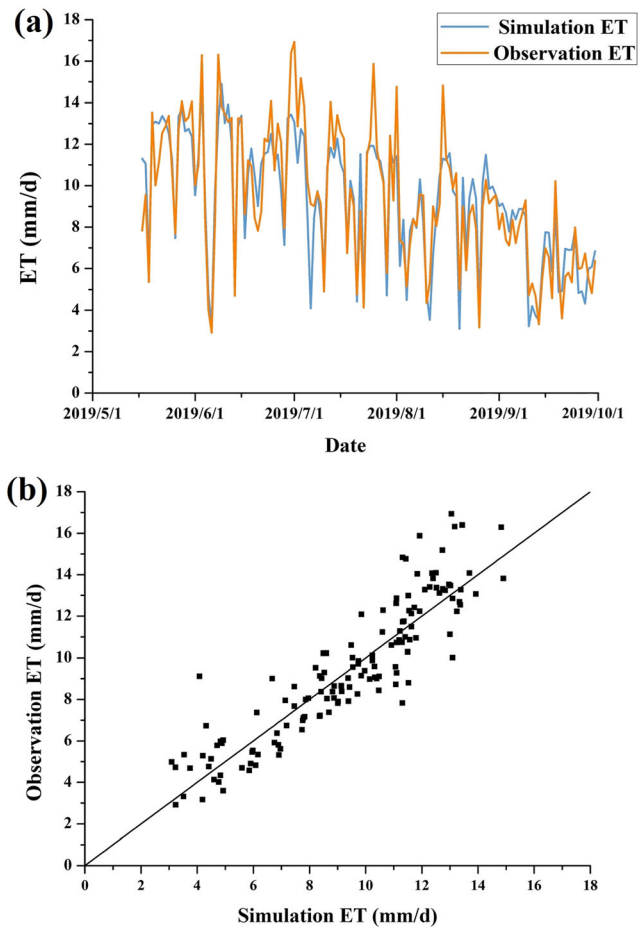
At the current groundwater level, the main soil water supply sources of the *P. australis* root layer in Lake Baiyangdian at different densities was upward replenishment from deep soil water. The water replenishment from deep soil was positively correlated with the vegetation density. At the same time, the rainfall infiltration replenishment (approximately 342 mm) was approximately half the replenishment rate from deep soil in the growing season. The total soil water replenishment under 0%, 20%, 40%, 60%, 80% and 100% density were 875 mm, 879 mm, 981 mm, 1126 mm, 1205 mm and 1337 mm, respectively. The main drainage methods of the root layer water over the whole growing season included plant transpiration, soil evaporation and deep leakage. Among these methods, the amount of deep leakage was the most stable among different densities. Transpiration increased with the increased density of *P. australis*, and the maximum transpiration was 1130 mm at 100% density. The trend of soil evaporation was the opposite, as the maximum, soil evaporation was 550 mm under the bare soil condition, and the minimum was 48 mm at 100% density (Table 4).

In general, during the growing season, all soil water balances of the 0–120 cm layer under each density condition of *P. australis* showed water accumulation (Table 4), and the discrepancy in accumulation amounts between different densities was small (all approximately 20–50 mm). The main reason for these results may be that with the proposal of the Xiong'an New District, the ecological environment of Lake Baiyangdian has been more effectively managed, and Lake Baiyangdian experienced considerable ecological water replenishment in 2018. The groundwater level in the study area

Fig. 6 Comparisons of the simulated and measured evapotranspiration for full-cover *P. australis*. (Observation *ET* represents the measured evapotranspiration (mm/d); simulation *ET* represents the simulation evapotranspiration of improved model (mm/d))

continued to rise, and the amount of water was sufficient. The amount of soil water consumed by evapotranspiration at different densities may be completely replenished by groundwater and rainfall over time. Eventually, the discrepancy in the balance of soil water content between different densities was small.
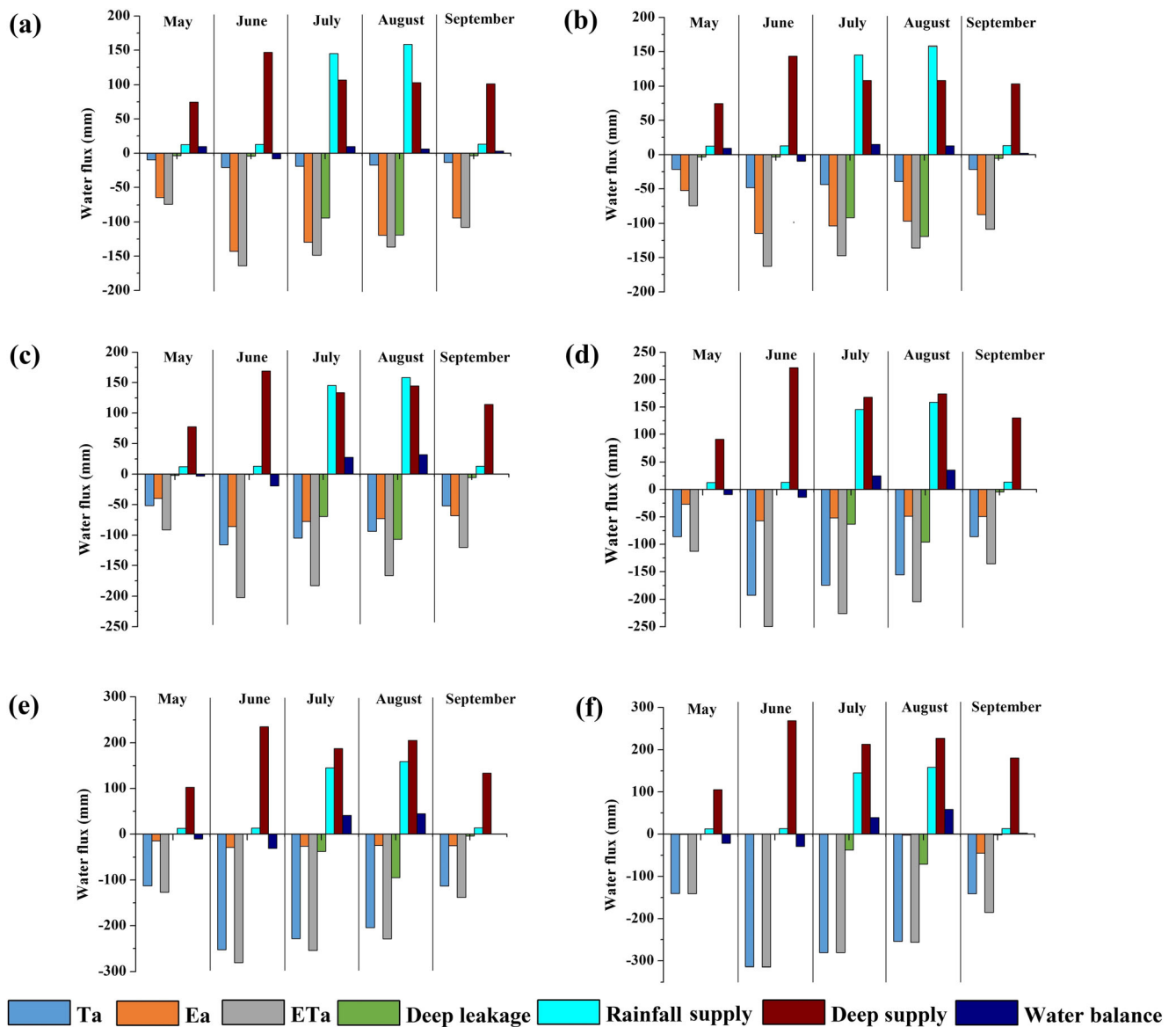
Monthly Water Flux Changes in the SPAC System Interface at Different Vegetation Densities

With the improved HYDRUS-DualKc model, at the monthly scale, the composition and variance of the water flux at the interface of the SPAC system at different vegetation densities was quantitatively analyzed (Fig. 7). The results showed that plant transpiration was unimodal during the growing season and consistent with the growth process of *P. australis*. The maximum value of transpiration under different density conditions all occurred in June and July except for bare land. For 100% density, the maximum value of soil evaporation occurred at the end of plant growth period (September); the main

Table3 Evapotranspiration simulation under different $K_{cb\ mid\ Table}$ scenarios

$K_{cb\ mid\ Table}$	R^2	NSE	Re (%)
2.1	0.80	0.76	12.47
2.2	0.83	0.79	12.27
2.3	0.83	0.83	12.36
2.4	0.83	0.82	13.54
2.5	0.83	0.78	15.56

$K_{cb\ mid\ Table}$ is the crop coefficient with a full coverage of vegetation in Baiyangdian; R^2 is the coefficient of determination; NSE is the Nash-Sutcliffe efficiency coefficient; Re is the relative deviation

Table 4 Water flux changes of 0–120 cm in the SPAC system interface at different vegetation densities

Vegetation density	T_a (mm)	E_a (mm)	ET_a (mm)	Deep leakage (mm)	Rainfall infiltration (mm)	Deep supply (mm)	ΔW (mm)
0%	–	550	550	225	342	533	20
20%	174	454	628	222	342	537	30
40%	418	344	762	183	342	639	38
60%	695	234	929	164	342	784	37
80%	912	118	1030	136	342	863	45
100%	1130	48	1178	110	342	995	50

T_a is actual vegetation transpiration; E_a is actual soil evaporation; ET_a is the actual evapotranspiration; ΔW is the soil water storage changes

Fig. 7 Monthly water flux changes of 0–120 cm in the SPAC system interface at different vegetation densities. ((**a**), (**b**), (**c**), (**d**), (**e**), (**f**) represent the *Phragmites australis* densities of 0%, 20%, 40%, 60%, 80% and 100%, respectively; T_a is actual vegetation transpiration. E_a is actual soil evaporation; ET_a is the actual evapotranspiration)

reason may be that soil exposure was increased with vegetation withering and the temperature was continuously high at the end of the vegetation period. Simultaneously, with the plants were withering their transpiration functions would also have diminished, leaving more water in the soil, and more water to be lost to soil evaporation. So evaporation tended to increase at the end of the vegetation period. Under different density conditions of *P. australis*, all the evapotranspiration values also showed a unimodal trend from May to September. The maximum value of evapotranspiration under different density conditions all occurred in June. In general, during each month, with the increase in the *P. australis* density, the proportion of transpiration increased and the proportion of evaporation decreased.

The supply relationships between different densities of *P. australis* were shown as Fig. 7. In May and June, for each density, the main water replenishment was a deep supply. In July and August, the main source was rainfall infiltration for low density (0%–40%) and deep supply for high density (60%–100%). In September, due to the decrease in rainfall, the supply source came from deep soil water again, and its value was approximately 90% of the total replenishment in September. Under the different density conditions, the total replenishment amount of the soil layer showed a unimodal trend from May to September, the maximum replenishment amount occurred in August. Water drainage of the root layer included plant transpiration, soil evaporation and deep leakage. The amount of deep leakage was stable between different densities; in May, June and September, the amount was low, while it was approximately 66 mm and 100 mm in July and August, respectively. However, the discrepancy of transpiration or evaporation between the different densities was large. Under the bare land conditions, the drainage method for soil water in each month was soil evaporation. For 20% vegetation density, the main drainage pathway in May, June, July and September was soil evaporation, and deep leakage in August. For 40% vegetation density, the main drainage pathway in May, June, July was transpiration, deep leakage in August, and evaporation in September. For the conditions of 60%–100% vegetation density, the main drainage pathway from May to September was plant transpiration. Under the different density conditions, the total drainage values of the soil layer from May to September were 78–140 mm, 166–314 mm, 239–318 mm, 255–327 mm, and 111–187 mm, respectively.

In general, at the current groundwater level, the discrepancy of the water balance among different densities and different months was shown in Fig. 7. In May and June, vegetation was in a fast-growing season and consumed considerable amounts of water, and there were few water supplements in the study area, thus, the soil water balance in May and June was loss. However, from July to September, with the increase in replenishment, the water balance in the soil layer was accumulating. From July to September, the average accumulation was a

monotonous trend, with the maximum in August and the minimum in September (Fig. 7).

Analysis of Water Transport and Dissipation in the SPAC System Interface in Different Groundwater Level Scenarios

To analyze water transport and dissipation with fluctuating groundwater levels, according to the current groundwater level, four groundwater level modelled scenarios were used for simulation (Table 5). According to the improved HYDRUS-DualKc model, vertical water transport and dissipation in multiple scenarios were simulated, which included the fluctuations of groundwater and different densities of *P. australis*. The simulation results are shown in Table 6. The groundwater level fluctuation affected the water requirement of *P. australis* and soil evaporation. As shown in Table 6, for 0%–60% density, the groundwater level fluctuation mainly contributed to changes in evaporation rather than changes in transpiration. For 80%–100% density, the groundwater level fluctuation mainly contributed to changes in transpiration rather than changes in evaporation, the main reason lay in that transpiration was one of main dissipative ways for the reed community during the growing season, therefore, the decrease of water content had a bigger influence on transpiration than evaporation. This result was consistent with results from previous research (Mazur et al. 2014). In the same vegetation density scenario, with the increase of the buried depth of the groundwater level, the actual evapotranspiration significantly decreased and was less than the potential evapotranspiration. For example, at 100% density, the total amount of evapotranspiration in the present scenario for the groundwater level was 1178 mm, while in scenario 4, it was 953 mm; this nearly 20% variation demonstrated that the fluctuation of the groundwater

Table 5 Groundwater level modelled scenarios

Date (mm-dd)	Groundwater level(cm)				
	Present	Scenario 1	Scenario 2	Scenario 3	Scenario 4
5–16	69.75	80	40	0	−20
5–31	60.42	80	40	0	−20
6–15	59.85	80	40	0	−20
6–30	48.55	80	40	0	−20
7–15	55.10	80	40	0	−20
7–31	67.17	80	40	0	−20
8–15	89.02	80	40	0	−20
8–31	105.42	80	40	0	−20
9–20	110.43	80	40	0	−20

The datum is at a 120 cm depth below the ground; Scenarios 1–4 are the buried depth of groundwater of 40 cm, 80 cm, 120 cm and 140 cm, respectively

Table 6 Water flux changes in the SPAC system interface in various vegetation densities in different groundwater level modelled scenarios

Scenario	Vegetation density	T_a (mm)	E_a (mm)	ET_a (mm)	vTop (mm)	vBot (mm)	ΔW (mm)
1	0%	0	550	550	208	303	15
	20%	174	454	628	112	303	18
	40%	418	344	763	2	443	25
	60%	695	234	929	−108	601	18
	80%	912	118	1030	−225	704	24
	100%	1133	48	1180	−295	862	27
2	0%	0	550	550	208	270	−18
	20%	174	454	628	112	270	−16
	40%	418	344	763	2	400	−18
	60%	695	234	929	−108	562	−23
	80%	863	96	959	−247	559	−54
	100%	1120	47	1167	−295	791	−36
3	0%	0	525	525	183	173	−90
	20%	172	381	552	38	119	−91
	40%	416	318	734	−24	292	−97
	60%	686	125	811	−218	373	−97
	80%	766	82	848	−261	382	−122
	100%	995	13	1008	−330	573	−99
4	0%	0	466	466	123	58	−144
	20%	171	324	495	−18	12	−140
	40%	414	251	665	−91	169	−150
	60%	673	101	774	−241	288	−142
	80%	733	81	814	−261	319	−154
	100%	940	13	953	−330	485	−132

T_a is actual vegetation transpiration; E_a is actual soil evaporation; ET_a is the actual evapotranspiration; vTop is the water flux of the upper interface (infiltration/evaporation: −/+); vBot is the water flux of the lower interface (inflow/outflow: +/-); ΔW is the soil water storage changes; Scenarios 1–4 are the average buried depth of groundwater of 80 cm, 90 cm, 110 cm and 120 cm, respectively

level had a great influence on evapotranspiration in the study area. At the same groundwater level, the total amount of evapotranspiration was positively correlated with the vegetation density. However, the increased amount from bare land to land with 100% density differed with the groundwater scenarios; this decrease was accompanied by an increased burial depth of the groundwater level. Therefore, from the perspective of water consumption of evapotranspiration, the vegetation density variations and groundwater level fluctuations all would affect the evapotranspiration of the area.

In the study area, in the same groundwater level scenario, the soil water storage changes (ΔW) of the root layer among different vegetation densities were similar (Table 6). However, at the same vegetation density, the soil water balance between different groundwater level scenarios was quite different. At the current groundwater level, the soil water balance was cumulative, and the cumulative amount was approximately 37 mm. In scenario 1, the soil water content of 0–120 cm during the growing season remained stable. However, in scenarios 2–4, the soil water content was at a deficit, and the

water deficit amount of the root layer increased with the raised burial depth of the groundwater level. When the average buried depth of the groundwater level increased to scenarios 2, 3 and 4, the soil water losses in the growing season were approximately 27 mm, 99 mm or 143 mm, respectively. Thus, to maintain the soil water balance, the groundwater level was kept above the groundwater level of scenario 1. Specifically, the average buried depth of the groundwater level remained at approximately 40 cm, which was beneficial to the balance of soil water of *P. australis* in the wetland. In general, from the perspective of the soil water balance in the wetland, the variations in groundwater level had an obvious influence on the soil water balance, while the variations of the vegetation density had little effect on the soil water balance. All these initiatives helped to expand our understanding of water transport and dissipation during groundwater level fluctuations and ecological pattern changes while also establishing suitable water management initiatives for the future.

In general, wetland ecological restorations, through the coupling of the relationship between vegetation patterns and

hydrological processes, have gradually become one of the important directions of ecological hydrology research of wetlands. Previous research has focused on the effects of vegetation types on the hydrological process, resulting in the lack of a comprehensive understanding of the interaction among water transport and dissipation, ecological processes and the vegetation structure in the wetland. This study proposed to construct an improved model (HYDRUS-DualKc model) suitable for vegetation density regulation, overcoming the shortcomings of vegetation density regulation in most models. The results of the model simulation may help us to understand the impact of vegetation density variations on water transport and dissipation. In addition, the effects of groundwater level fluctuations were important for water transport and dissipation in the SPAC. In this research, the results showed that the groundwater level fluctuations had a high impact on the water transport and dissipation in Lake Baiyangdian. Moreover, compared with vegetation density variations, groundwater level fluctuations not only affected evapotranspiration but also affected the soil water balance in the wetland. Therefore, a reasonable water resource allocation required effective management of the groundwater level. In actual management, accurate estimations of water transport and dissipation are important prerequisites for the efficient use of regional water resources, especially in semi-arid areas. Therefore, this research can provide foundation technical support for the sustainable management of regional water resources and ecological landscapes.

Conclusions

In this paper, an improved model was constructed, it based on the HYDRUS and dual crop coefficient models for simulating the water transport and dissipation at different vegetation densities and different groundwater levels. Then, supported by field measurements, the responses of the vertical water transport and dissipation that included evapotranspiration, the water supply and drainage and the water balance to changes in the groundwater level and different *P. australis* densities were explored using the improved model. In general, from the perspective of the water consumption of evapotranspiration, both vegetation density variations and groundwater level fluctuations would affect the evapotranspiration. For 0%–60% density, the groundwater level fluctuation mainly contributed to changes in evaporation rather than changes in transpiration. For 80%–100% density, the groundwater level fluctuation mainly contributed to changes in transpiration rather than changes in evaporation. From the perspective of the water supplement and drainage, the main water replenishment source of soil water of different *P. australis* densities in the same month was very same, but the drainage relationship was inconsistent. From the perspective of the soil water balance,

the fluctuation in groundwater level had an obvious influence on the soil water balance, while the variations in vegetation density had relatively small effects on the soil water balance.

This study can provide an improve method for evaluating water transport and dissipation at different interfaces and overcame the difficulty of daily-scale continuous monitoring of these dynamics in SPAC systems at different vegetation densities. The provided model could better represent the dynamics that was expected from our knowledge of hydrological and ecological theory. These results can assist in understanding the responses of water transport and dissipation at the interfaces of atmosphere-vegetation, atmosphere-soil and the vegetation root layer to the vegetation pattern and hydrological regime. Additionally, the results of this study can make up for the lack of systematic research on the water transport process within the groundwater-soil-plant-atmosphere continuum in the *P. australis* community of Lake Baiyangdian. Finally, the results of this research can be used to help maintain the lake ecosystem health, efficient use of regional water resources and inform the optimal allocation of water resources and ecological water supplements in this semi-arid region. However, this study only simulated water transport and dissipation in raised fields and generalized the issue into a vertical one-dimensional one. At the same time, water surface evaporation in the wetland area also plays an important role in the regional water cycle. Due to the wetland rainfall, surface water, soil water, plant water and groundwater being closely related, the source of replenishment was not only rainfall and deep soil water but also surface water replenishment. Therefore, future research needs to explore the wetland's regional water transport and dissipation by conversion from a point scale to a surface scale for effective environmental management.

References

Allen RG, Pereira LS, Raes D, Smith M (1998) Crop evapotranspiration-guidelines for computing crop water requirements- FAO irrigation and drainage paper 56. Food and Agriculture Organization, Rome

Amiri E (2017) Evaluation of water schemes for maize under arid area in Iran using the SWAP model. Communications in Soil Science and Plant Analysis 48:1963–1976

Baird AJ (1999) Eco-hydrology - plants and water in terrestrial and aquatic environments - introduction. In Baird AJ, Wilby RL (Eds.), *Routledge Physical Environment Series* (1-10). (reprinted)

Barreto CEAG, Wendland E, Marcuzzo FFN (2009) Estimating evapotranspiration based on groundwater level variation in a watershed. Engenharia Agrícola 29:52–61

Borin M, Milani M, Salvato M, Toscano A (2011) Evaluation of Phragmites australis (Cav.) Trin. Evapotranspiration in northern and southern Italy. Ecological Engineering 37:721–728

Brix H, Sorrell BK, Lorenzen B (2001) Are Phragmites-dominated wetlands a net source or net sink of greenhouse gases? Aquatic Botany 69:313–324

Chen L, Wang J, Wei W, Fu B, Wu D (2010) Effects of landscape restoration on soil water storage and water use in the loess plateau region, China. Forest Ecology and Management 259:1291–1298

Chesson P, Gebauer R, Schwinning S, Huntly N, Wiegand K, Ernest M, Sher A, Novoplansky A, Weltzin JF (2004) Resource pulses, species interactions, and diversity maintenance in arid and semi-arid environments. Oecologia 141:236–253

Cortina J, Amat B, Castillo V, Fuentes D, Maestre FT, Padilla FM, Rojo L (2011) The restoration of vegetation cover in the semi-arid Iberian southeast. Journal of Arid Environments 75:1377–1384

Drexler JZ, Snyder RL, Spano D, Paw K (2004) A review of models and micrometeorological methods used to estimate wetland evapotranspiration. Hydrological Processes 18:2071–2101

Fahle M, Dietrich O (2014) Estimation of evapotranspiration using diurnal groundwater level fluctuations: comparison of different approaches with groundwater lysimeter data. Water Resources Research 50:273–286

Fu W, Huang M, Gallichand J, Shao M (2012) Optimization of plant coverage in relation to water balance in the loess plateau of China. Geoderma 173-174:134–144

Goodwin I, Whitfield DM, Connor DJ (2006) Effects of tree size on water use of peach (Prunus persica L. Batsch). Irrigation Science 24:59–68

Gribovszki Z, Kalicz P, Szilagyi J, Kucsara M (2008) Riparian zone evapotranspiration estimation from diurnal groundwater level fluctuations. Journal of Hydrology 349:6–17

Herbst M, Kappen L (1999) The ratio of transpiration versus evaporation in a reed belt as influenced by weather conditions. Aquatic Botany 63:113–125

Hoffman GJ, Genuchten MTV (1983) Soil properties and efficient water use: water management for salinity control. In: Taylor HM, Jordan WR, Sinclair TR (eds) Limitations and efficient water use in crop production. American Society of Agronomy, Madison

Jefferson LV (2004) Implications of plant density on the resulting community structure of mine site land. Restoration Ecology 12:429–438

Jiang J, Feng S, Huo Z, Zhao Z, Jia B (2011) Application of the SWAP model to simulate water-salt transport under deficit irrigation with saline water. Mathematical and Computer Modelling 54:902–911

Karimov AK, Simunek J, Hanjra MA, Avliyakulov M, Forkutsa I (2014) Effects of the shallow water table on water use of winter wheat and ecosystem health: implications for unlocking the potential of groundwater in the Fergana Valley (Central Asia). Agricultural Water Management 131:57–69

Li F, Ma Y (2019) Evaluation of the dual crop coefficient approach in estimating evapotranspiration of drip-irrigated summer maize in Xinjiang, China. Water 11:1053–1069

Li Y, Simunek J, Jing L, Zhang Z, Ni L (2014) Evaluation of water movement and water losses in a direct-seeded-rice field experiment using Hydrus-1D. Agricultural Water Management 142:38–46

Liu B, Shao M (2015) Modeling soil-water dynamics and soil-water carrying capacity for vegetation on the loess plateau, China. Agricultural Water Management 159:176–184

Lortie CJ, Turkington R (2002) The effect of initial seed density on the structure of a desert annual plant community. Journal of Ecology 90:435–445

Ludwig JA, Wilcox BP, Breshears DD, Tongway DJ, Imeson AC (2005) Vegetation patches and runoff-erosion as interacting ecohydrological processes in semiarid landscapes. Ecology 86:288–297

Mastrocicco M, Colombani N, Salemi E, Castaldelli G (2010) Numerical assessment of effective evapotranspiration from maize plots to estimate groundwater recharge in lowlands. Agricultural Water Management 97(9):1389–1398

Mazur MLC, Wiley MJ, Wilcox DA (2014) Estimating evapotranspiration and groundwater flow from water-table fluctuations for a general wetland scenario. Ecohydrology 7:378–390

Moiwo JP, Yang Y, Li H, Han S, Yang Y (2010) Impact of water resource exploitation on the hydrology and water storage in Baiyangdian Lake. Hydrological Processes 24:3026–3039

Poblete-Echeverría CA, Ortega-Farias SO (2013) Evaluation of single and dual crop coefficients over a drip-irrigated merlot vineyard (Vitis viniferaL.) using combined measurements of sap flow sensors and an eddy covariance system. Australian Journal of Grape and Wine Research 19:249–260

Ritchie JT (1972) Model for predicting evaporation from a row crop with incomplete cover. Water Resources Research 8:1204

She D, Liu D, Xia Y, Shao M (2014) Modeling effects of land use and vegetation density on soil water dynamics: implications on water resource management. Water Resources Management 28:2063–2076

Wang S, Fu BJ, Gao GY, Yao XL, Zhou J (2012a) Soil moisture and evapotranspiration of different land cover types in the loess plateau, China. Hydrology and Earth System Sciences 16:2883–2892

Wang F, Wang X, Zhao Y, Yang Z (2012b) Long-term water quality variations and chlorophyll a simulation with an emphasis on different hydrological periods in lake Baiyangdian, northern China. Journal of Environmental Informatics 20:90–102

Wang X, Su J, Cai Y, Tan Y, Yang Z, Wang F (2013) An integrated approach for early warning of water stress in shallow lakes: a case study in Lake Baiyangdian, North China. Lake and Reservoir Management 29:285–302

Wang F, Wang X, Zhao Y, Yang Z (2014a) Temporal variations of NDVI and correlations between NDVI and hydro-climatological variables at Lake Baiyangdian, China. International Journal of Biometeorology 58:1531–1543

Wang F, Wang X, Zhao Y, Yang Z (2014b) Correlation analysis of NDVI dynamics and hydro-meteorological variables in growth period for four land use types of a water scarce area. Earth Science Informatics 7:187–196

Xu X, Zhang Q, Li Y, Li X (2016) Evaluating the influence of water table depth on transpiration of two vegetation communities in a lake floodplain wetland. Hydrology Research 47:293–312

Zhang YK, Schilling KE (2006) Effects of land cover on water table, soil moisture, evapotranspiration, and groundwater recharge: a field observation and analysis. Journal of Hydrology 319:328–338

Zhao P, Li S, Li F, Du T, Tong L, Kang S (2015) Comparison of dual crop coefficient method and Shuttleworth-Wallace model in evapotranspiration partitioning in a vineyard of Northwest China. Agricultural Water Management 160:41–56

Zhong P, Yang Z, Cui B, Liu J (2005) Studies on water resource requirement for eco-environmental use of the Baiyangdian wetland. Acta Scientiae Circumstantiae 25:1119–1126

Zhou L, Zhou G (2009) Measurement and modelling of evapotranspiration over a reed (Phragmites australis) marsh in Northeast China. Journal of Hydrology 372:41–47